Journal of Cleaner Production 116 (2016) 187–197

Contents lists available at ScienceDirect

Journal of Cleaner Production

journal homepage: www.elsevier.com/locate/jclepro

Specific energy based evaluation of machining efficiency

Vincent A. Balogun [a, *], Isuamfon F. Edem [b], Adefemi A. Adekunle [c], Paul T. Mativenga [b]

[a] College of Engineering, Department of Mechanical & Mechatronics Engineering, Afe Babalola University, Ado Ekiti, Nigeria
[b] School of Mechanical, Aerospace and Civil Engineering, The University of Manchester, Manchester M13 9PL, United Kingdom
[c] Department of Mechatronics Engineering, Federal University Oye Ekiti, Nigeria

ARTICLE INFO

Article history:
Received 11 April 2015
Received in revised form
18 December 2015
Accepted 29 December 2015
Available online 7 January 2016

Keywords:
Ploughing energy
Swept angle
Undeformed chip thickness
Specific energy
Process waste
Machining efficiency

ABSTRACT

Rubbing and ploughing increase the tool tip energy demand in machining. An efficient set of cutting conditions would direct the energy into material shearing and hence selecting the efficient set is a value adding activity. In this work, a side milling tests were conducted on a milling machine tool to investigate the specific ploughing energy on AISI 1045 steel alloy, titanium 6Al–4V alloy and aluminium AW6082-T6 alloy materials. The relationship between the cutter swept angle and the specific ploughing energy is explored. An optimised model for width of cut and undeformed chip thickness at which ploughing effect would be minimal is proposed. The proposed methodology can be used to evaluate machining efficiency based on maximum specific shear energy and also to derive the specific ploughing energy for minimum tip energy demand.

1. Introduction

1.1. The total specific energy and chip morphology

The electrical energy input into machining processes can cater for material shearing (Gutowski et al., 2006), ploughing and friction (Guo and Chou, 2004), new surface generation and chip momentum change (Kalpakjian and Schmid, 2003) and machine tool energy losses and process upkeep (Lucca et al., 1991). The modelling of specific energy in machining relates to the tip energy (Anderberg et al., 2010; Diaz et al., 2011; Balogun and Mativenga, 2013) i.e. the energy required for actual material removal (Li and Kara, 2011). Since the surface energy and the momentum energy represent a very small and negligible amount compared to the specific frictional and specific shear energies, and also because they do not contribute to chip removal processes, they are incorporated into the specific ploughing energy (Arsecularatne, 1997). Therefore, the total specific cutting energy K_e in J/mm^3 can be categorised as in Equation (1).

$$K_e = k_f + k_p + k_s \quad (1)$$

where K_e is the total specific cutting energy, k_f represents the specific friction energy in J/mm^3; k_p is the specific ploughing energy in J/mm^3 and k_s is the specific shearing energy in J/mm^3.

The estimated value of the specific cutting energy varies for different machining processes even when the workpiece material properties remain the same. For example, the specific cutting energy of grinding operations is higher compared to other machining processes like turning and milling (Ghosh et al., 2008). This is due to the inefficient nature of the abrasive grit in grinding compared to the use of defined cutting edges as in other mechanical machining processes. The knowledge of specific energy can be important (Ghosh et al., 2008) because for example, the specific cutting energy in grinding operations influences surface integrity of machined components (Paul and Chattopadhyay, 1995) especially in ductile materials and is one of the characteristics of ploughing effect. Drazumeric et al. (2014) also documented the need to determine the specific energy of the workpiece during grinding operations. Bifano and Fawcett (1991) reported that specific grinding energy is a useful process parameter for the control of grinding ductility since the specific grinding energy is accompanied by a transition from ductile-regime grinding to brittle-regime grinding. Sarwar et al. (2009) reported that specific cutting energy is one of the better ways of quantitatively measuring the

* Corresponding author.
E-mail address: balogunav@abuad.edu.ng (V.A. Balogun).

http://dx.doi.org/10.1016/j.jclepro.2015.12.106
0959-6526/

efficiency of the metal cutting process or the machinability of a workpiece material.

Ploughing effect can be explained as the action of the cutting tool pushing the material (especially at undeformed chip thickness lower than the cutting edge radius) upwards and/or side ways to form a ridge-like structure and burrs on top, at the entry, exit or side of the machined surfaces depending on the type of machining operations.

The consumed electrical energy demand for ploughing is undesirable. This is because often, no desired work is done and this is a waste of energy (with the exception of grinding operations) since; the ploughed materials remain attached to the workpiece material after the tool pass. This effect is indicated by the surface integrity realised after the tool pass (DeVor and Kapoor, 2004; Aramcharoen and Mativenga, 2009). Ploughing effect has also been identified to affect the geometrical accuracy of machined products (Gillespie, 1979; Lee and Dornfeld, 2005; Aramcharoen and Mativenga, 2009). Therefore, it is desirable to reduce or if possible eliminate the specific ploughing energy in mechanical machining processes. Ploughing is encouraged by a lower ratio of undeformed chip thickness to the cutting edge radius. This scenario is known as 'size effect' in mechanical machining processes. Size effect plays an important role in manufacturing processes and determines the changes that affect the process behaviour (Vollertsen et al., 2009).

Lucca et al. (1993) used ploughing and elastic spring back effect to explain the increase in specific cutting energy. In a previous work, Lucca et al. (1991) used the relation between the undeformed chip thickness and the cutting edge radius to explain the transition from shearing dominated machining process to ploughing dominated process. The authors further reported that in ploughing dominated machining processes, the force per unit width in the thrust direction was found to increase more rapidly than the force per unit width in the cutting direction. This implies that the tool edge condition has a significant effect on the thrust forces when the depth of cut was below the tool edge radius. In this case, rubbing phenomenon is predominant and this resulted in higher friction forces at the tool–chip interface (Waldorf, 2006). Increase in cutting forces means a corresponding increase in specific cutting energy.

In the study on brass materials, Taminiau and Dautzenberg (1991) reported an increased specific cutting energy when machining at an undeformed chip thickness less than the cutting edge radius. The average specific cutting energy was almost constant when the ratio of the undeformed chip thickness to the cutting edge radius is equal or more than unity.

Singh et al. (2011b) in their analysis and study of specific ploughing energy for mild steel and composite ceramics during a grinding operation deduced an equation for the specific ploughing energy using single grit scratch test (Singh et al., 2011a). They reported that the specific ploughing energy was a significant component of total specific grinding energy which is responsible for around 40–80% of the specific grinding energy. This was found to dominate at low depth of cut especially with materials of hard and high strength such as conductive ceramic.

1.2. Process mechanisms in mechanical machining operations

Chip formation is a good indication of material characteristics and the machinability of workpiece materials. It has been shown that chip formation not only depends on material characteristic and cutting tool geometry, but also on the ratio of feed per tooth to cutting edge radius (Lucca et al., 1993; Aramcharoen and Mativenga, 2009; Balogun and Mativenga, 2014). Chae et al. (2006) show that this ratio is between 5% and 35% of the tool edge radius. At a value below the minimum chip thickness, no chip will be formed and the process will be dominated by rubbing and ploughing. This is an indication of high frictional force at the tool–chip contact interface and plastic deformation of the cutting tool as a result of high temperature (Kim et al., 2004; Ducobu et al., 2009).

Researchers explained that the machining process mechanisms were dominated by rubbing, ploughing and shearing (Bissacco et al., 2006; Ducobu et al., 2009). For example, Chae et al. (2006), Ducobu et al. (2009) and Aramcharoen and Mativenga (2009) use the relationship between undeformed chip thickness and cutting tool edge radius in orthogonal cutting process to define the three established mechanisms during a mechanical machining process. These are as depicted in Fig. 1.

Fig. 1 shows the relationship between cutting edge radius and the undeformed chip thickness during a machining process. The first scenario occurs when the undeformed chip thickness h, is less than the cutting edge radius r_e (i.e. the ratio h/r_e is less 1). In this case, the cutter will deform elastically and the workpiece material will be compressed by the cutting tool. Material spring back effect is dominant where workpiece material is forced under the cutting tool and then recovers back after the tool passes as shown in Fig. 1a. The cutting mechanism at this zone is dominated by rubbing and ploughing effect (Bissacco et al., 2006) and as a result of this phenomenon, cutting and frictional forces increases rapidly (Ducobu et al., 2009), rake angle will also increase as a result of materials gathering around the cutting tool edge radius which will increase the chip thickness (Lee and Dornfeld, 2005). This will eventually cause an increase of specific cutting energy.

In the second scenario (Fig. 1b) where the ratio h/r_e is approximately equal to 1, the process mechanism consist effect of ploughing and shearing. The process mechanism tends to move from a rubbing and ploughing dominated area to a shearing dominated zone. However still, the effect of ploughing exists at this zone and shearing effect tends to be more dominant (Ducobu et al., 2009). Although a chip is formed, the workpiece material undergoes an elastic deformation and recovery at the desired depth of cut after the tool pass. Thus, the removed material is less than the desired value giving rise to a poor dimensional accuracy and surface integrity.

Fig. 1c show the third scenario. In this zone, the ratio h/r_e is greater than 1. The elastic deformation of the workpiece decreases rapidly and an improved chip is formed. In this zone, the process mechanism tends to be value adding and sustainable machining. A lower specific energy demand is an expected characteristic in this zone and an indication of the efficiency of the process.

Other force components, for example the ploughing force components, are neglected either because they cannot be measured or they do not contribute to chip formation processes and considered too small. The ploughing force is difficult to be isolated from the measured force data (Guo and Chou, 2004) and rubbing and ploughing mechanisms are notably significant in tool wear assessment and monitoring, material flow stress calculation, chip formation mechanisms (Zulaika et al., 2011), and machined surface integrity. The impact of the process mechanisms ultimately affects the tool tip energy demand of the process. The process mechanisms can also be used to define the efficiency of the machining operations. In the case where rubbing and ploughing are said to be dominant, the process is within the 'Waste' dominated zone since no chips are removed from the workpiece. On the other hand, if the process is dominated by shearing effect, then it can be said to be a 'Value adding' operations. Therefore, and from literature, for a machining operation to be energy centric, efficient and sustainable, it should be within the value adding zone. A zone whereby rubbing and ploughing effect are reduced and/or eliminated and shearing effect encouraged. This research work is

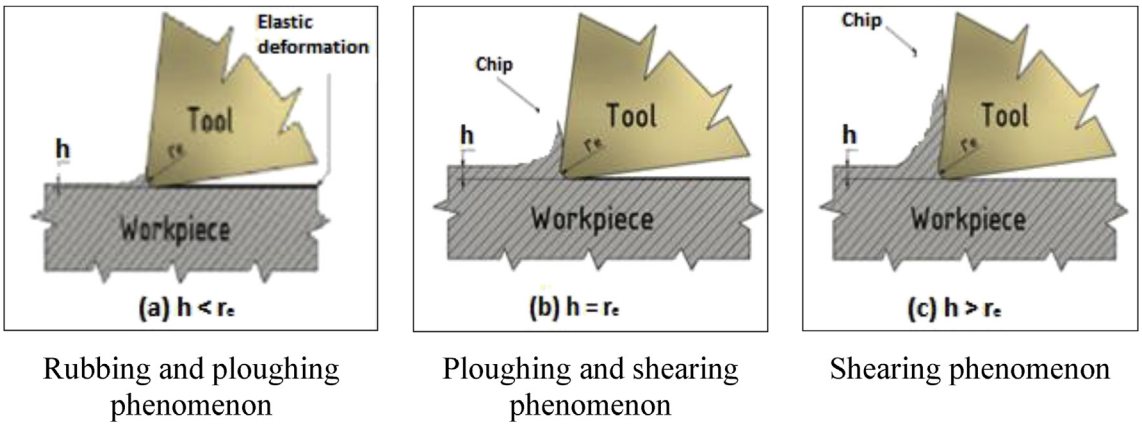

Fig. 1. Effect of undeformed chip thickness ratio to the cutting edge radius in orthogonal cutting adapted from Aramcharoen and Mativenga (2009).

motivated to test this overstretched hypothesis for validity. Hence, the needs for this research work.

1.3. Research aim and objective

The aim of this work is to investigate the process mechanism during milling operations. This was to enable the identification of process parameters and evaluate process efficiency at which the mechanisms of rubbing, ploughing and shearing effect are dominant. The study also aimed to propose a methodology to estimate the specific ploughing energy (by which the shear energy can be deduced) and optimise cutter engagement. The result will enable process and system designers to optimise electrical energy usage for resource efficiency and sustainable manufacture of products.

2. Experimental set up and methodology

2.1. Cutter swept angle optimisation and their influence on specific ploughing energy in milling processes

In order that the optimised radial depth of cut is engaged, a pilot test was carried out on AISI 1045 steel alloy. A general purpose TiAlN coated carbide single insert SOMT-060204-HQ with geometry shown in Table 1 was used for the side milling test. The milling test was conducted on a high speed Mikron HSM 400 machining centre under a dry cutting environment. The electrical current consumption was measured with a FLUKE 345 power clamp meter. The FLUKE 345 power clamp meter was clamped on the main cable (at the back of the machine) that supplies electricity current to the machine tool. This was used to record the electricity consumption during the side milling tests. The power consumption during the side milling tests were evaluated from the average of the electrical current measured with the FLUKE 345 power clamp meter. This study was to investigate the correlation between the radial depth of cut and ploughing effect during a milling operation.

The cutting tool edge radius was visualised and estimated under the Leica DM2500M Microscope. The edge radius was measured by inserting a best fit circle that intersects the tangential line drawn across the rake and flank faces of the insert. The dimension of the circle (i.e. cutting edge radius) was automatically evaluated by the microscope. Fig. 2 is a representation of how the cutting edge radius was evaluated. The measured values are as shown in Table 2 and the average of the three values (approximated to 60 μm) represents the cutting edge radius employed for this work.

For this experiment, the radial depth of cut a_e, feed rate, and depth of cut were varied as shown in Table 3. The side milling test was conducted in such a way that each test engaged a different cutter swept angle. The cutter swept angles and the undeformed chip thicknesses were estimated with Equations (2) and (3) (Boothroyd and Knight, 1989) respectively considering the radial depth of cut for each set of milling test.

$$\cos \varnothing = \frac{r_n - a_e}{r_n} \tag{2}$$

where $\varnothing$ is the cutter swept angle in degrees, r_n is the cutter radius in mm and a_e is the cutter engagement or step over in mm.

$$h_{m(avg)} = \frac{f_z}{\varnothing_s} \int_0^{\varnothing} \sin \varnothing \, d\varnothing \tag{3}$$

Table 1
Cutting tool geometry.

Geometry	Values
Nose radius (mm)	0.4
Edge radius (μm)	60
Positive rake angle (degrees)	5
Rake face primary chip breaker land (μm)	60
Clearance angle (degrees)	7

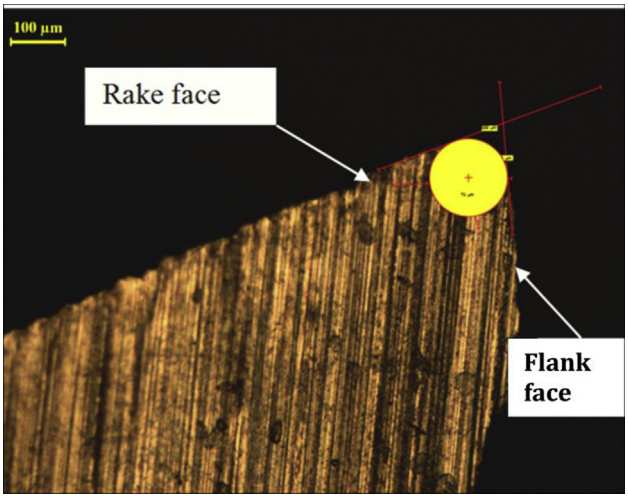

Fig. 2. Cutting edge radius measurement under Leica DM2500M Microscope.

Table 2
Average cutting edge radius measured under Leica DM2500M Microscope.

Insert nomenclature	Measured tool edge radius, r_e (μm)			Average (μm)
	1	2	3	
SOMT-060204-HQ	56.8	62.5	59.6	59.6

Table 3
Cutting parameters for AISI 1045 steel alloy.

Feedrates (mm/min)	62	621	1179	2855	3413
Feed f_z (mm/tooth)	0.01	0.10	0.19	0.46	0.55
Radial depth of cut a_e (mm)	0.20	0.40	0.60	0.80	1.00

where $h_{m(avg)}$ is the average undeformed chip thickness in mm, f_z is the feed in mm/tooth, $\varnothing_s$ is the cutter swept angle in radians.

The radial depth of cut a_e (i.e. 0.20, 0.40, 0.60, 0.80 and 1.00 mm) equates to cutter swept angles of 18.2°, 25.8°, 31.8°, 36.9 and 41.4° evaluated with Equation (2). Cutting tests were carried out with each of the swept angle kept constant while varying the feed in turn. For example, a constant radial depth of cut of 0.2 mm in combination with each of the feed shown in Table 3 (i.e. 0.01, 0.10, 0.19, 0.46 and 0.55 mm/tooth respectively) were adopted in turn for the cutting test. Each of the tests was repeated three times for consistency and repeatability of the result obtained. The total power demand for each test were recorded and plotted against the material removal rate as shown in Fig. 3 in order to determine the specific energy coefficient machining AISI 1045 steel alloy. This procedure is also in line with the work of Uriarte et al. (2008).

Fig. 3 shows the relationship between power demand and material removal rate during side milling operations of AISI 1045 steel alloy.

The specific energy coefficient is represented by the slope of the power–material removal rate trend line and tabulated in Table 4. It was observed that as the cutter swept angle increases, the specific energy reduces varying from 7.80 to 1.56 J/mm^3. This is due to the fact that the milling test gradually moved from smaller to higher chip thickness and from a ploughing dominated area to a shearing dominated one. From Table 4, it can be deduced that the ratio of h/r_e increases from 0.033 to 3.167 (i.e. r_e = 60 μm). For ratio of h/r_e = 0.033, the specific energy coefficient obtained is 7.80 J/mm^3 and decreases to 1.56 J/mm^3 for the side milling test conducted on the AISI 1045 steel alloy material. Higher specific energy values were reported to indicate the effect of rubbing and ploughing (i.e. size effect) during the cutting experiment and lower range of specific energy is a transition to shearing dominated cutting (Ducobu et al., 2009; Bissacco et al., 2006). Therefore, it can be deduced that to reduce ploughing effect in milling processes, a higher cutter swept angle must be engaged.

Analysing further, the relationship between specific energy coefficients was plotted against the cutter swept angles. The result shows a non-linear relationship. It can be seen from Fig. 4 that at lower cutter swept angles 18.2° (a_e of 0.2 mm), the specific energy was 7.80 J/mm^3 while the values decreases to a value of 1.56 J/mm^3 for cutter swept angle 41.4°. The lower range of specific energy values is relatively comparable to published values in literature (Kalpakjian and Schmid, 2003).

Following on from Fig. 4, a quadratic trend curve fitted well with R^2 of 0.98. The nonlinear relationship was defined by a quadratic equation because only one visible bend (hills and valleys) appeared in the curved line (i.e. gradual decreasing order). The regression equation derived from Fig. 4 is stated in Equation (4).

Differentiating the regression equation:

$$k = 0.0128(CSA)^2 - 1.0173(CSA) + 21.911 \quad (4)$$

Differentiating Equation (4) with respect to the cutter swept angle;

$$\frac{dk}{d\varnothing} = 0 = 0.0256(CSA) - 1.0173 \quad (4b)$$

$$\varnothing_{opt} = 39.74^\circ \quad (4c)$$

It can be seen that the optimum cutter swept angle for minimising the specific energy for the insert nose radius of 0.4 mm used is 39.74°. At this angle, the shearing effect will be dominant since the ratio h/r_e is greater than 1. The specific cutting energy is therefore at an optimised value when compared with a lower cutter swept angle of 18.2°. Hence, the step over which equates to the optimum specific cutting energy can be estimated.

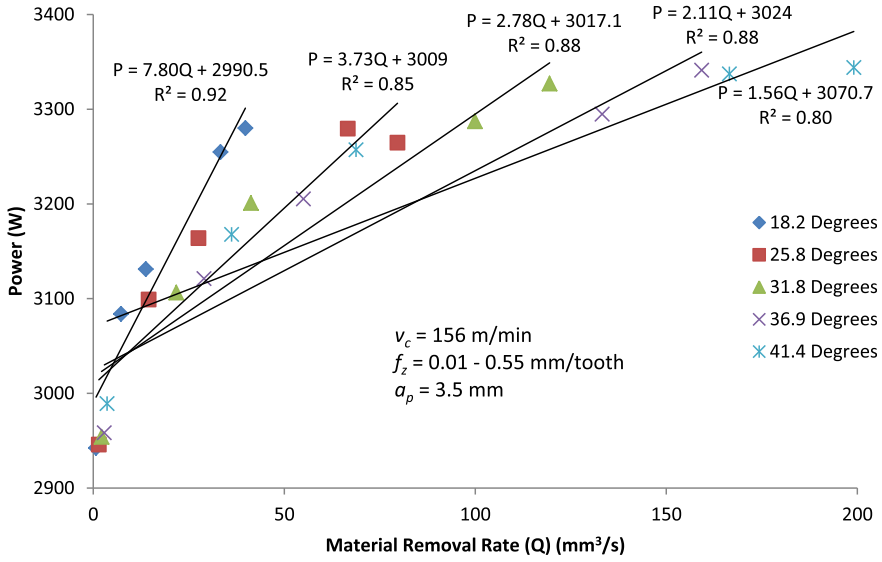

Fig. 3. Power–material removal rate graph at different cutter swept angle when machining AISI 1045 steel alloy.

Table 4
Specific energy coefficient data for AISI 1045 steel alloy obtained from tests.

f_z (mm/tooth)	h_m Average (mm)	Cutter swept angle (CSA) (degrees)	k (J/mm^3)
0.010	0.002	18.2	7.80
0.100	0.022	25.8	3.73
0.190	0.051	31.8	2.78
0.460	0.143	36.9	2.11
0.550	0.190	41.4	1.56

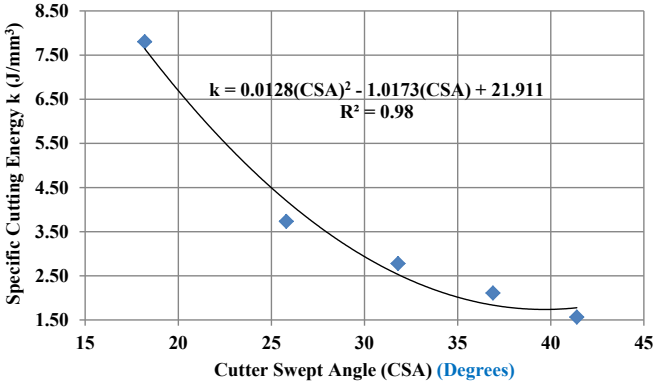

Fig. 4. Optimum cutter swept angle.

From Fig. 5, the average undeformed chip thickness is defined as in Equation (3) and the cutter swept angle deduced based on Equation (2).

From Equations (2) and (4c), the cutter engagement can be estimated thus:

$$\begin{aligned} a_e &= r_n - r_n \cos \varnothing \\ a_e &= r_n(1 - \cos 39.74^\circ) \\ a_e &= 0.23 r_n \end{aligned} \tag{5}$$

From this case study, the cutter diameter was 8 mm, and the experimental optimum cutter swept angle was 39.74°, it therefore follows from Equation (5) that the optimum cutter engagement should be 0.92 mm offset. Also, from Fig. 5 and Equation (3), the undeformed chip thickness can be estimated as stated in Equation (6).

$$\frac{h_{max}}{f_z} = \sin \varnothing = \sin 39.74^\circ = 0.64 \tag{6}$$

$$\begin{aligned} h_{max} &= 0.64 \times f_z \\ &= \text{Optimised maximum undeformed chip thickness} \end{aligned} \tag{6b}$$

where h_{max} is the maximum undeformed chip thickness in mm, f_z is the chip load in mm/tooth and a_e is the step over or the radial depth of cut in mm.

Although the specific energy of the reported optimum swept angle of 39.74° might be worse than that of the 41.4°, it is important to note that there is trade-offs between surface integrity and specific energy demand values that relate process efficiency.

In order to further validate the existence of trade-offs between the surface integrity and specific energy that relates to the choice of the quadratic trend curve shown in Fig. 4, the machined surface integrity of the AISI 1045 were measured with the Optical Microscope and visualised with the Map Vue EX-Surface Mapping Software version 6.55. Figs. 6 and 7 show the surface maps and the plot of the swept angles against the average surface roughness respectively.

It was observed that as the swept angle increases, the average surface roughness tends towards and exceeded the recommended value of 1.60 μm (as indicated by line AB in Figs. 7 and 8) by the International Standard Organization (ISO), 3685 (ISO, 3685). The specific energy values evaluated from each of the swept angles were then plotted against the average surface roughness as shown in Fig. 8.

From Fig. 8 it can be seen that as the specific energy demand decreases (from 5.38 kJ/mm^3 to 1.65 kJ/mm^3), the average surface roughness increases up to 1.73 μm within the investigated swept angles. Since it has been recommended by the International

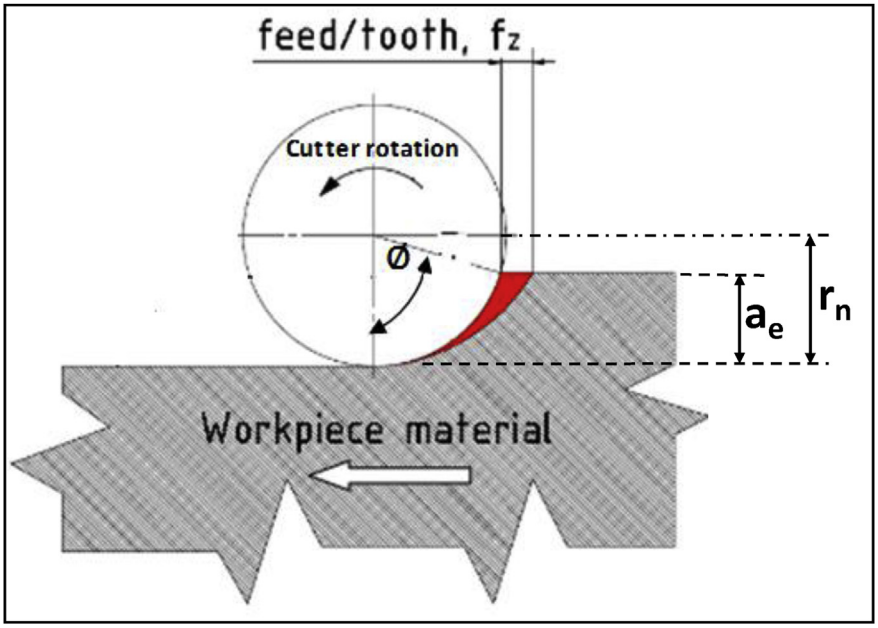

Fig. 5. Cutter engagement with workpiece.

Standard Organization (ISO), 3685 that the average surface roughness value for machining should not exceed 1.60 μm, a value above this range were ignored in selecting the optimum swept angle for minimum specific energy demand. However, further decrease in specific energy might be considered as the best minimum specific energy demand for process efficiency but the measured surface roughness renders this point unsustainable. Therefore, for minimum specific energy demand that yields the acceptable surface roughness, the specific energy should not be less than 1.65 kJ/mm^3 as shown in Fig. 8. This value equates to surface roughness as indicated by line AB in Figs. 7 and 8. Hence the optimum swept angle obtained lies within the acceptable 1.60 μm recommended surface roughness. It can therefore be deduced that the minimum specific energy does not translate to optimum process efficiency. The trade-offs between specific energy and the surface integrity must be considered. This is the selection criteria for adopting the optimum swept angles deduced with Equation (4).

The optimum swept angle of 39.74° deduced through the quadratic trend line in Equation (4) gave a range of surface roughness values below 1.60 μm recommended by the ISO 3685. However, other minimum specific energy is recorded when the swept angles exceed 39.74°. The surface roughnesses measured when the swept angles exceeds 39.74° are outside the recommended values for surface integrity. It then follows that an optimum swept angle that gave minimum specific energy and also within the acceptable surface integrity of 1.60 μm is adopted as

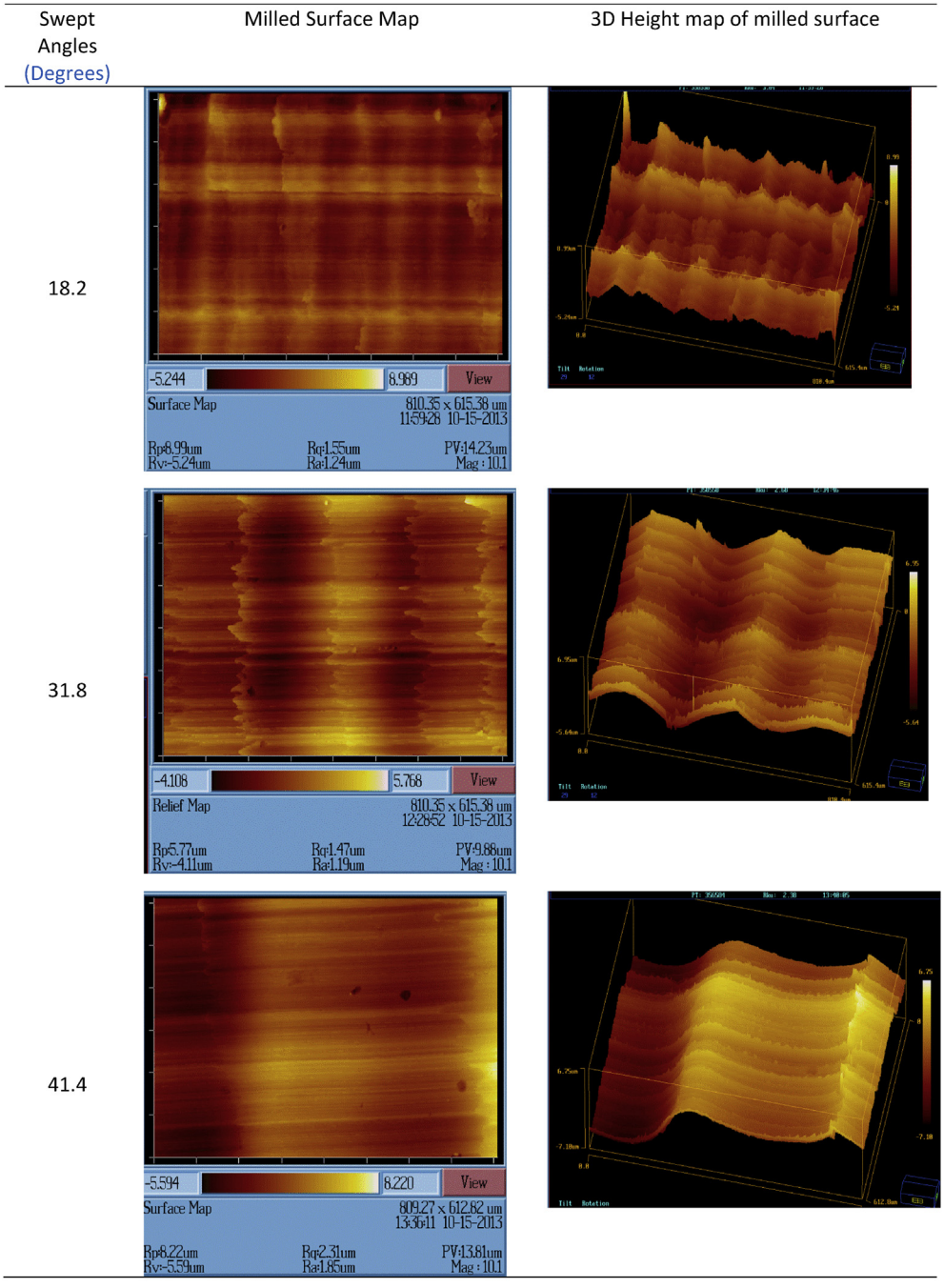

Fig. 6. Surface integrity maps of AISI 1045 alloy steel machined at different swept angles.

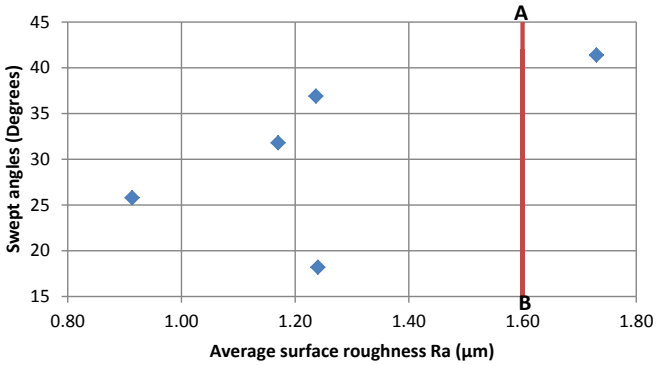

Fig. 7. Impact of swept angles on surface roughness after milling AISI 1045 alloy steel.

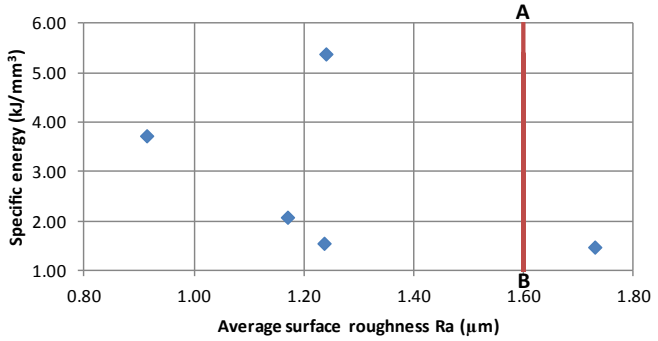

Fig. 8. Specific energy and surface roughness trade-off after milling AISI 1045 alloy steel.

39.74°. This also supports the argument for the adoption of a quadratic trend curve fitted in Fig. 4 and stated in Equation (4).

The optimum swept angle was obtained in order to further determine the parameter variations for the evaluation of the specific energy and process efficiency. Hence, for optimised values of the specific cutting energy that would improve process efficiency, the step over a_e should not be less than $0.23 \times r_n$ and the maximum undeformed chip thickness should not be less than $0.64 \times f_z$ as shown in Equations (5) and (6b) respectively. This equation agrees with Campatelli et al. (2014), when they reported that the optimal value of the radial engagement (i.e. radial width of cut) to minimise the specific energy that is related only to the efficiency of cutting is achieved by maintaining the value suggested by the tool manufacturer, about 1 mm and at that value, the feed per tooth shows an optimal design value for a 0.12 mm/tooth. For example, in comparing Campatelli et al. (2014) results and from Equation (6b) (assuming feed/tooth is 0.12 mm/tooth), it therefore implies that the undeformed chip thickness is equal to 0.077 mm. This also implies that the ratio of the undeformed chip thickness to cutting edge radius is equivalent to 1.28 (cutting edge radius of insert used is 0.06 mm from Table 1). This value also correlates to the point at which the effect of shearing dominates the rubbing and ploughing effect. The specific energy at this point is expected to be comparably lower when compared to the rubbing–ploughing dominated machining.

In order to estimate the machining process efficiency that would distinguish the value adding and waste processes, an understanding of the process mechanism is necessary. This will enable the process to be adequately categorised and evaluated. Therefore, the milling experiment was designed with the understanding that the specific energy is increased when step over $\ll 0.23r_n$ and $h \ll 0.64f_z$. This range of values would adequately account for the specific energy controlled by the process mechanisms i.e. rubbing, ploughing and shearing. This range of values also defines value adding and waste criterion of the process.

Since the impact of the ploughing effect is increased at values of a_e and f_z less than the proposed values, the ranges of values for the step over were set to overlap the proposed values. Hence, the step over was set at $0.063r_n$, $0.125r_n$, $0.188r_n$ and $0.25r_n$. This value equates to cutter swept angles of 20.36°, 28.96°, 35.66° and 41.41°. The value of f_z was set at 0.01, 0.10, 0.19, 0.28, 0.37, 0.46 and 0.55 mm/tooth. These values equates to undeformed chip thickness h of 0.003, 0.035, 0.066, 0.097, 0.128, 0.159 and 0.190 mm respectively as shown in Table 5. These ranges would allow the milling to be carried out within the ploughing and shearing domain so that a clearer picture of the ploughing effect could be observed and properly represented on the specific energy variation curve.

2.2. Estimation of the specific ploughing energy

With knowledge of the optimised cutter engagement and undeformed chip thickness values, a side milling test was conducted on aluminium AW6082-T6 alloy, AISI 1045 steel alloy and titanium 6Al–4V alloy under the Mikron HSM 400 machining centre with a spindle HVC140-SB-10-15/42-3FHSK-E40 and Heidenhain TNC 410 NC controller. A general purpose multi-layered TiAlN coated carbide single insert SOMT-060204-HQ with geometry as in Table 1 was mounted on a tool holder E90X-D08-C10-06 with an overhang of 25 mm. The cutting parameters and chemical composition of the workpiece materials were as stated in Table 5. The machining tests were conducted under a dry cutting environment. Each workpiece materials of size 50 mm × 100 mm × 3.5 mm was clamped and supported by parallel slips on a milling vice. The material overhang was limited to 12 mm just enough to accommodate a set of machining test and to eliminate the effect of vibrations of the workpiece materials during the machining process. Each milling test was repeated three times in order to test for repeatability and consistency of the data collated. A new cutting tool edge was introduced for a new set of tests in order that the cutting tool wear characteristics was not introduced into the electrical current measured. The electrical current consumption was measured with a FLUKE 345 Power Clamp meter. The side milling tests were conducted based on the procedure published by Balogun and Mativenga (2014).

In order for that the specific ploughing energy be properly accounted for, an analysis based on the work of Balogun and Mativenga (2014) was adopted and the specific energy coefficient values derived based on the optimised cutter swept angle and undeformed chip thickness analysis reported in Section 2.1.

The specific energy coefficients obtained on three different workpiece material was as shown in Table 6. It can be seen that at a lower feed for example 0.010 mm/tooth, the specific energy coefficients were 13.08, 10.66 and 5.31 J/mm^3 for aluminium AW6082-T6 alloy, titanium 6Al–4V alloy and AISI 1045 steel alloy respectively.

The higher values of specific energy at such undeformed chip thickness is a result of the contribution of ploughing effect at which rubbing, higher frictional effect and plastic deformation of the cutting tool dominate. From Fig. 9, it is shown that as the undeformed chip thickness increases, the ploughing effect tends to decrease and eventually eliminated as the feed increases. This phenomenon is not the same for all machining processes. For example, in micro-machining where components are miniaturised, ploughing effect cannot be avoided since the ratio of undeformed chip thickness to the cutting edge radius is always less than unity. However, with adequate knowledge of the range of specific energies, an optimised value of the undeformed chip thickness can be

Table 5
Workpiece materials and cutting parameters for milling trials.

	Aluminium alloy AW6082-T6	AISI 1045	Titanium alloy 6Al–4V
Feed (mm/tooth)	0.01–0.55	0.01–0.55	0.01–0.55
Undeformed chip thickness h (μm)	0.003–0.190	0.003–0.190	0.003–0.190
Depth of cut (mm)	3.5	3.5	3.5
Cutting velocity (m/min)	210	156	80
Radial depth of cut (mm)	0.25–1.00	0.25–1.00	0.25–1.00
Tool diameter (mm)	8	8	8
Chemical composition (maximum)	95.35% Al, 1% Mn, 0.5% Fe, 1.2% Mg, 1.3% Si, 0.1% Cu, 0.2% Zn, 0.1% Ti, 0.25% Cr	96.96% Fe, 0.46% C, 0.40% Si, 0.65% Mn, 0.40% Cr, 0.10% Mo, 0.40% Ni, 0.63% Others	89.37% Ti, 6% Al, 4% V, 0.08% C, 0.3% Fe, 0.2% O, 0.05% N
Material hardness	HV 100	HV 146.4	HV 329

estimated to avoid catastrophic wear and/or damage of the cutting tools. This will cause an improvement on the surface integrity of the machined component and also reduce the values of specific ploughing energy.

3. Proposed analysis of the specific ploughing energy

The specific energy coefficients obtained for AISI 1045 steel alloy, aluminium AW6082-T6 alloy, and titanium 6Al–4V alloy respectively were plotted against the ratio of the undeformed chip thickness to the cutting edge radius for the three materials under investigation. Figs. 10–12 show the contribution of ploughing effect on the specific energy curves.

From Fig. 9 two distinctive regions can be observed. The first region is where the undeformed chip thickness is less than the cutting edge radius. At this region, it is observed that higher values of specific energy resulted. This is due to the influence of ploughing effect. At this point also, the spring back effects are pronounced and diminutive or no chips are formed (Nasr et al., 2007; Woon et al., 2008; Mian et al., 2011). The boundary is a point where the ratio of undeformed chip thickness and the cutting edge equals unity and the second region is a near constant trend zone of specific energy values where the undeformed chip thickness is greater than the cutting edge radius.

In micro, nano and pico machining, the cutting plane usually falls within the first region where ploughing is dominant thereby an increase in the tool tip energy will be observed. Whereas, in the case of macro-machining, the cutting plane lies within the third region where shearing is dominant and the values of the specific energy recorded agrees with that available from literature (Kalpakjian and Schmid, 2003).

Figs. 10–12 show that at higher value of undeformed chip thickness, for example above 66 μm for AISI 1045 steel alloy, the relationship between specific energy and h/r_e is more or less linear. The tool edge radius was 60 μm. Therefore fitting a straight trend line AB to the experimental data curve for h > 66 μm and

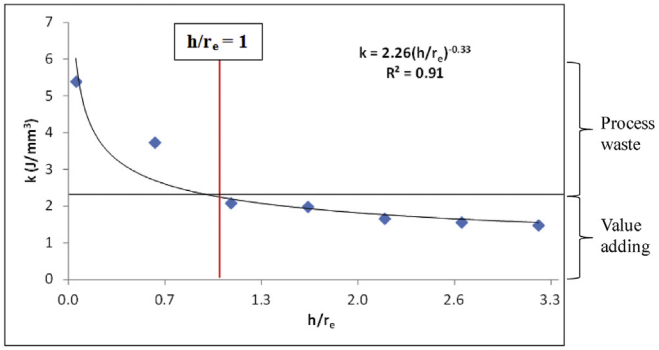

Fig. 9. Impact of size effect on specific cutting energy for dry cutting AISI 1045 steel alloy.

extrapolating to $h/r_e = 0$, gives a value which can be interpreted as the point of maximum shear. Therefore the intercepted point A gives a value equivalent to the maximum specific shear energy of 2.25, 2.42 and 4.91 J/mm^3, for aluminium AW6082-T6 alloy, AISI 1045 steel alloy and titanium 6Al–4V alloy respectively as depicted in Figs. 10–12. Machining processes conducted within these range of values are called the "Value-adding process".

The trend line Equations (7)–(9) of line AB shown in Figs. 10–12, represent the maximum specific shear energy equations at which ratio h/r_e equals zero.

$$k_{S(\max)} = 2.42 - 0.32\left(h/r_e\right) \tag{7}$$

$$k_{Al(\max)} = 2.25 - 0.71\left(h/r_e\right) \tag{8}$$

Table 6
Experimental specific energy coefficient values.

Cutting variables			Material		
			AISI 1045	Aluminium alloy	Titanium alloy
f_z (mm/tooth)	v_c (m/min)	a_p (mm)	Specific energy coefficient (J/mm^3)		
0.01	156	3.5	5.31	13.08	10.66
0.10			3.73	1.99	4.45
0.19			2.08	1.52	3.28
0.28			1.97	0.78	2.55
0.37			1.65	0.87	2.65
0.46			1.55	0.21	1.14
0.55			1.47	0.21	1.13

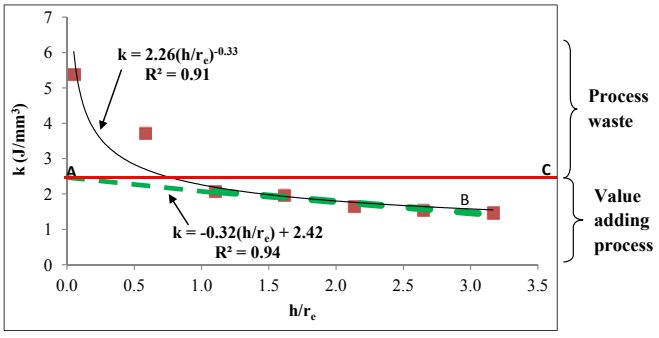

Fig. 10. Shear energy estimation of AISI 1045 steel alloy.

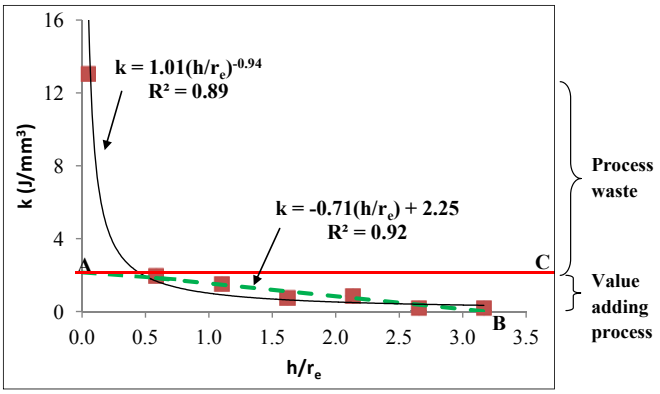

Fig. 11. Shear energy estimation of aluminium AW6082-T6 alloy.

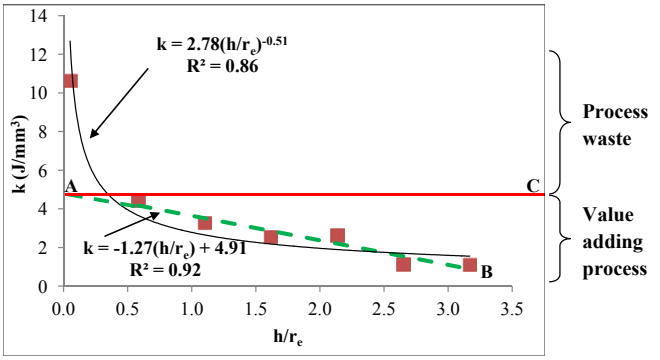

Fig. 12. Shear energy estimation of titanium 6Al–4V alloy.

$$k_{T(\max)} = 4.91 - 1.27\left(h/r_e\right) \tag{9}$$

where $k_{S(max)}$, $k_{Al(max)}$ and $k_{T(max)}$ represent maximum specific shear energy of AISI 1045 steel alloy, aluminium AW6082-T6 alloy and titanium 6Al–4V alloy respectively in J/mm^3.

It also can be deduced that a specific energy value above line AC indicates effects of ploughing mechanisms (also could include rubbing) and termed "Process waste" zone. For example during the cutting tests and at f_z of 0.01 mm/tooth, the total specific energy calculated was 5.31, 10.66 and 13.08 J/mm^3 (Table 6) for AISI 1045 steel alloy, titanium 6Al–4V alloy and aluminium AW6082-T6 alloy respectively. At these ranges of values, the ratio h/r_e tends towards zero (cutting edge radius $r_e = 0.06$ mm). This means that the bulk of the specific energy is due to ploughing mechanisms and infinitesimally small rubbing mechanisms. It can be deduced therefore that the specific ploughing energy is 54%, 54% and 83% of the total specific energy demand for AISI 1045 steel alloy, titanium 6Al–4V alloy and aluminium AW6082-T6 alloy respectively (these values are true for cutting test conducted at a feed of 0.01 mm/tooth). This percentage gradually decreases as the ratio h/r$_e$ increases more than unity. These values also confirm the work of Singh et al. (2011b) where they reported that ploughing effects contribute to about 40–80% of the total specific cutting energy in mechanical machining processes.

This value can be said to be true since ploughing effect dominates as values of $h/r_e \ll 0$ or approaches an infinitesimal values. Therefore the difference between the maximum specific shear energy and the experimental maximum value is equivalent to the total specific ploughing energy used up due to the size effect for side milling the workpiece materials under investigation.

Therefore, from Figs. 10–12 the area below the linear trend line AB indicates an area at which the process mechanisms are optimised and is said to be the value adding zones. Comparatively, area above the maximum specific shear (line AC) indicates higher specific energy (i.e. increased ploughing and rubbing mechanisms) hence termed process waste zone. For the purpose of sustainability and resource efficiency, it is therefore recommended that machining operations be conducted within area within the maximum specific shear line AC. This area can be estimated for different workpiece materials as proposed in this paper.

The process mechanism model can therefore be deduced from the above analysis as shown in Fig. 13 for AISI 1045 steel alloy, aluminium AW6082-T6 alloy and titanium 6Al–4V alloy respectively. The process mechanism model can be used to further describe the cutting characteristics depicted in Figs. 10–12. The process mechanism includes three mechanisms i.e. rubbing, ploughing and shearing. The mechanisms engaged during a mechanical machining operation are dependent on type of cutting operations and the ratio h/r_e.

Looking at the graphs at Figs. 10–12 the specific cutting energy showed an exponential increase when ratio of undeformed chip thickness to the cutting edge radius is less than unity and approaches zero. In this zone, the effective rake angle is predominantly negative and ploughing and rubbing are the dominant process mechanisms. It can therefore be inferred that higher specific energies are correlated to process inefficiency through rubbing and shearing.

The above result shows that at lower ratio h/r$_e$, the specific ploughing energy is higher more than 50% of the specific energy required for milling any workpiece materials. More so, the values become higher with ductile materials. For example for aluminium AW6082-T6 alloy, this could be above 60%. The result further confirms the work of Schaller et al. (1999) and Mian et al. (2010) that the specific ploughing energy is relatively higher in ductile materials. This methodology can be applied to determine maximum specific shear energy demand and specific ploughing energy for machining.

In analysing the process mechanisms, the impact of ploughing and rubbing was quantified based on the average specific shear energy required to create a value adding operation. This was achieved by assuming a range of values for the ratio h/r_e from 0.01 to 2 and substituting their values into, for example, Equation (7) for AISI 1045 steel alloy. The effect of rubbing and ploughing can hence be shown as in Fig. 13 for AISI 1045 steel alloy, aluminium AW6082-T6 alloy and titanium 6Al–4V alloy respectively.

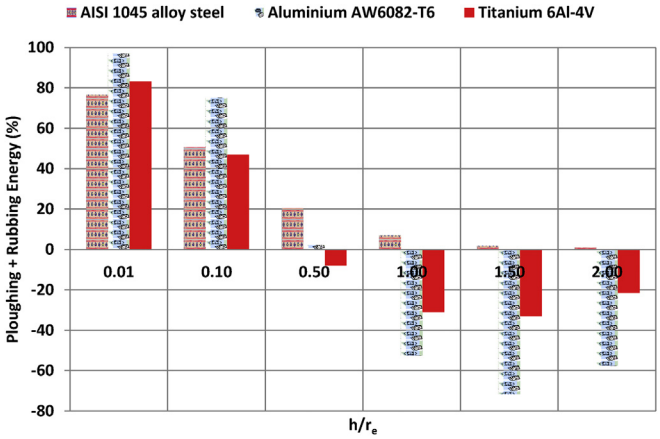

Fig. 13. Ploughing energy variations with process parameter for AISI 1045 steel alloy, aluminium AW6082-T6 alloy and titanium 6Al–4V alloy.

This energy demand value is an indicator of the efficiency of the machining operation engaged. For example, it can be seen from Fig. 13 that as the ratio of undeformed chip thickness to the cutting edge radius increases from 0.01 to 2 and above for AISI 1045 steel alloy, the percentage of the ploughing and rubbing effects gradually decreases from 78% to 5%. This is a further proof that in order to improve the efficiency of a machining operation and at low tip energy demand, the ploughing effect should be reduced or eliminated if possible. However, since the machining processes are a combination of roughening and finishing, the effect of ploughing might not be eliminated or ignored. For example, in grinding operation whereby the grit size of the grinding wheel is oftentimes equal to or less than the chip thickness, the ploughing energy could be considerably higher compared to other machining operations.

Assuming machining AISI 1045 alloy steel with $h/r_e = 1$ (i.e. undeformed chip thickness and cutting edge radius are both 0.06 mm); then the optimised specific energy for milling AISI 1045 will be 2.26 J/mm^3 as previously shown in Fig. 5. The estimate for the specific energy was derived using the power function equation obtained from the specific energy-h/r_e.

4. Conclusion

In this study, a new optimised value at which ploughing is minimum was found. This value corresponds to 39.74° cutter swept angle when machining with a tool that has an edge radius of 60 μm. This is so because at this angle, the process mechanism is within the shearing dominated zone and the value of $h/r_e = 1$. This value was derived for different workpiece materials and cutting parameters. Other conclusions derived from the study include:

- The specific ploughing energy can be estimated with the proposed methodology of extrapolation of the specific energy curve to the point where h/r_e is zero.
- The specific shear energy is 52%, 63.8% and 69% for AISI 1045 steel alloy, titanium 6Al–4V alloy and aluminium AW6082-T6 alloy respectively when compared to the specific energy values.
- In order to improve the process efficiency in mechanical machining, shearing dominated machining should be encouraged.
- From this work, it has been shown that machining efficiency is linked to process waste and value adding mechanisms, and shearing dominated cutting is optimum when h/r_e equals to 1. Also, the specific shear energy evaluated for the three materials under investigation shows that at lower ratio h/r_e, the specific ploughing energy is higher by more than 50% of the specific energy required for milling any of the three workpiece materials. Therefore, it can be concluded that at shearing dominated zone, the waste due to ploughing and rubbing could be reduced by over 50%. Hence the machining efficiency can be improved by over 50% without compromise to workpiece surface integrity by controlling tool step over to reduce the energy wasted in rubbing and ploughing.
- A pre-knowledge of the values of the specific ploughing energy can aid pre-process planning and support energy resource management.
- Size effect (as govern by the ratio h/r_e) has tremendous influence on the process mechanisms and by implication on the surface integrity of machined component. Therefore it is important to select optimum h/r_e ratio for minimum energy demand that would not compromise the surface integrity of the finished product.
- For sustainable and energy smart machining strategy that will promote cleaner production, it is important that manufacturers should consider machining at the shearing dominated zone. This will promote green manufacturing and resource efficiency.
- For energy centric machining, it is important to consider the trade-offs between the specific energy and surface integrity. This in some cases negates the adoption of the minimum energy criterion rules. However, it would promote machining sustainability and finish product acceptability within the international standards.

References

Anderberg, S.E., Kara, S., Beno, T., 2010. Impact of energy efficiency on computer numerically controlled machining. Proc. Inst. Mech. Eng. Part B J. Eng. Manuf. 224, 531–541.

Aramcharoen, A., Mativenga, P., 2009. Size effect and tool geometry in micromilling of tool steel. Precis. Eng. 33, 402–407.

Arsecularatne, J., 1997. On tool–chip interface stress distributions, ploughing force and size effect in machining. Int. J. Mach. Tools Manuf. 37, 885–899.

Balogun, V.A., Mativenga, P.T., 2013. Modelling of direct energy requirements in mechanical machining processes. J. Clean. Prod. 41, 179–186.

Balogun, V.A., Mativenga, P.T., 2014. Impact of undeformed chip thickness on specific energy in mechanical machining processes. J. Clean. Prod. 69, 260–268.

Bifano, T.G., Fawcett, S.C., 1991. Specific grinding energy as an in-process control variable for ductile-regime grinding. Precis. Eng. 13, 256–262.

Bissacco, G., Hansen, H.N., De Chiffre, L., 2006. Size effects on surface generation in micro milling of hardened tool steel. CIRP Ann.-Manuf. Technol. 55, 593–596.

Boothroyd, G., Knight, W., 1989. Fundamentals of Machining and Machine Tools. Marcel Dekker, New York.

Campatelli, G., Lorenzini, L., Scippa, A., 2014. Optimization of process parameters using a response surface method for minimizing power consumption in the milling of carbon steel. J. Clean. Prod. 66, 309–316.

Chae, J., Park, S., Freiheit, T., 2006. Investigation of micro-cutting operations. Int. J. Mach. Tools Manuf. 46, 313–332.

DeVor, R.E., Kapoor, S.G., 2004. On the modeling and analysis of machining performance in micro-endmilling, part I: surface generation. J. Manuf. Sci. Eng. 126 (4), 685–694.

Diaz, N., Redelsheimer, E., Dornfeld, D., 2011. Energy consumption characterization and reduction strategies for milling machine tool use. In: Hesselbach, J., Herrmann, C. (Eds.), Glocalized Solutions for Sustainability in Manufacturing. Springer, Berlin, Heidelberg, pp. 263–267.

Drazumeric, R., Badger, J., Krajnik, P., 2014. Geometric, kinematical and thermal analyses of non-round cylindrical grinding. J. Mater. Process. Technol. 214 (4), 818–827.

Ducobu, F., Filippi, E., Rivière-Lorphèvre, E., 2009. Chip formation and minimum chip thickness in micro-milling. In: Proceedings of the 12th CIRP Conference on Modelling of Machining Operations, pp. 339–346.

Ghosh, S., Chattopadhyay, A., Paul, S., 2008. Modelling of specific energy requirement during high-efficiency deep grinding. Int. J. Mach. Tools Manuf. 48, 1242–1253.

Gillespie, L., 1979. Deburring precision miniature parts. Precis. Eng. 1, 189–198.

Guo, Y., Chou, Y., 2004. The determination of ploughing force and its influence on material properties in metal cutting. J. Mater. Process. Technol. 148, 368–375.

Gutowski, T., Dahmus, J., Thiriez, A., 2006. Electrical energy requirements for manufacturing processes. In: 13th CIRP International Conference on Life Cycle Eng., Leuven, Belgium, p. 623.

ISO, 3685, 1993. Tool-life Testing with Single Point Turning Tools, ISO 3685:1993(E), second ed. International Organization for Standards, Geneva.

Kalpakjian, S., Schmid, S., 2003. Manufacturing Processes for Engineering Materials. Prentice-Hall, Englewood Cliffs, New Jersey.

Kim, C.J., Mayor, J.R., Ni, J., 2004. A static model of chip formation in microscale milling. Trans. ASME-B-J. Manuf. Sci. Eng. 126, 710–718.

Lee, K., Dornfeld, D.A., 2005. Micro-burr formation and minimization through process control. Precis. Eng. 29, 246–252.

Li, W., Kara, S., 2011. An empirical model for predicting energy consumption of manufacturing processes: a case of turning process. Proc. Inst. Mech. Eng. Part B J. Eng. Manuf. 225, 1636–1646.

Lucca, D., Rhorer, R., Komanduri, R., 1991. Energy dissipation in the ultraprecision machining of copper. CIRP Ann.-Manuf. Technol. 40, 69–72.

Lucca, D., Seo, Y., Komanduri, R., 1993. Effect of tool edge geometry on energy dissipation in ultraprecision machining. CIRP Ann.-Manuf. Technol. 42, 83–86.

Mian, A.J., Driver, N., Mativenga, P.T., 2010. A comparative study of material phase effects on micro-machinability of multiphase materials. Int. J. Adv. Manuf. Technol. 50, 163–174.

Mian, A.J., Driver, N., Mativenga, P.T., 2011. Identification of factors that dominate size effect in micro-machining. Int. J. Mach. Tools Manuf. 51, 383–394.

Nasr, M.N.A., Ng, E.G., Elbestawi, M.A., 2007. Modelling the effects of tool-edge radius on residual stresses when orthogonal cutting AISI 316L. Int. J. Mach. Tools Manuf. 47, 401–411.

Paul, S., Chattopadhyay, A., 1995. A study of effects of cryo-cooling in grinding. Int. J. Mach. Tools Manuf. 35, 109–117.

Sarwar, M., Persson, M., Hellbergh, H., Haider, J., 2009. Measurement of specific cutting energy for evaluating the efficiency of bandsawing different workpiece materials. Int. J. Mach. Tools Manuf. 49, 958–965.
Schaller, T., Bohn, L., Mayer, J., Schubert, K., 1999. Microstructure grooves with a width of less than 50 μm cut with ground hard metal micro end mills. Precis. Eng. 23, 229–235.
Singh, V., Durgumahanti, U.P., Rao, P.V., Ghosh, S., 2011a. Specific ploughing energy model using single grit scratch test. Int. J. Abras. Technol. 4, 156–173.
Singh, V., Ghosh, S., Rao, P.V., 2011b. Comparative study of specific plowing energy for mild steel and composite ceramics using single grit scratch tests. Mater. Manuf. Process. 26, 272–281.
Taminiau, D., Dautzenberg, J., 1991. Bluntness of the tool and process forces in high-precision cutting. CIRP Ann.-Manuf. Technol. 40, 65–68.
Uriarte, L., Azcarate, S., Herrero, A., De Lacalle, L.L., Lamikiz, A., 2008. Mechanistic modelling of the micro end milling operation. Proc. Inst. Mech. Eng. Part B J. Eng. Manuf. 222 (1), 23–33.
Vollertsen, F., Biermann, D., Hansen, H.N., Jawahir, I.S., Kuzman, K., 2009. Size effects in manufacturing of metallic components. CIRP Ann.-Manuf. Technol. 58 (2), 566–587.
Waldorf, D.J., 2006. A simplified model for ploughing forces in turning. J. Manuf. Process. 8, 76–82.
Woon, K.S., Rahman, M., Fang, F.Z., Neo, K.S., Liu, K., 2008. Investigations of tool edge radius effect in micromachining: a FEM simulation approach. J. Mater. Process. Technol. 195, 204–211.
Zulaika, J.J., Campa, F.J., de Lacalle, L.L., 2011. An integrated process–machine approach for designing productive and lightweight milling machines. Int. J. Mach. Tools Manuf. 51 (7), 591–604.